

# **Thiacalixarenes with sulfur functionalities at lower rim: heavy metal ion binding in solution and 2D-confined space**

Anton Muravev<sup>1,\*</sup>, Ayrat Yakupov<sup>2</sup>, Tatiana Gerasimova<sup>1</sup>, Daut Islamov<sup>1</sup>, Vladimir Lazarenko<sup>3</sup>, Alexander Shokurov<sup>4</sup>, Alexander Ovsyannikov<sup>1</sup>, Pavel Dorovatovskii<sup>3</sup>, Yan Zubavichus<sup>5</sup>, Alexander Naumkin<sup>4,6</sup>, Sofiya Selektor<sup>4</sup>, Svetlana Solovieva<sup>1</sup>, and Igor Antipin<sup>2</sup>

<sup>1</sup>Arbuzov Institute of Organic and Physical Chemistry, FRC Kazan Scientific Center, Russian Academy of Sciences, Arbuzov str. 8, 420088 Kazan, Russia

<sup>2</sup>Butlerov Institute of Chemistry, Kazan Federal University, Kremlevskaya str. 18, 420008 Kazan, Russia

<sup>3</sup>National Research Centre “Kurchatov Institute”, Kurchatov Square 1, 123182 Moscow, Russia

<sup>4</sup>Frumkin Institute of Physical Chemistry and Electrochemistry, Russian Academy of Sciences, Leninskii pr. 31, 119071 Moscow, Russia

<sup>5</sup>Synchrotron Radiation Facility SKIF, Boreskov Institute of Catalysis, Siberian Branch, Russian Academy of Sciences, Nikolskii pr. 1, 630559 Koltsovo, Russia

<sup>6</sup>Nesmeyanov Institute of Organoelement Compounds, Russian Academy of Sciences, Vavilov str. 28, 119334 Moscow, Russia

\*E-mail: antonm@iopc.ru

## **Electronic Supplementary Information**

### **Table of Contents:**

DLS measurements	S2
Crystallographic data	S2
Spectrophotometric titration data	S3
Analysis of frontier molecular orbitals	S4
Langmuir monolayer measurements	S5
XPS spectra	S6
Copies of NMR spectra	S7

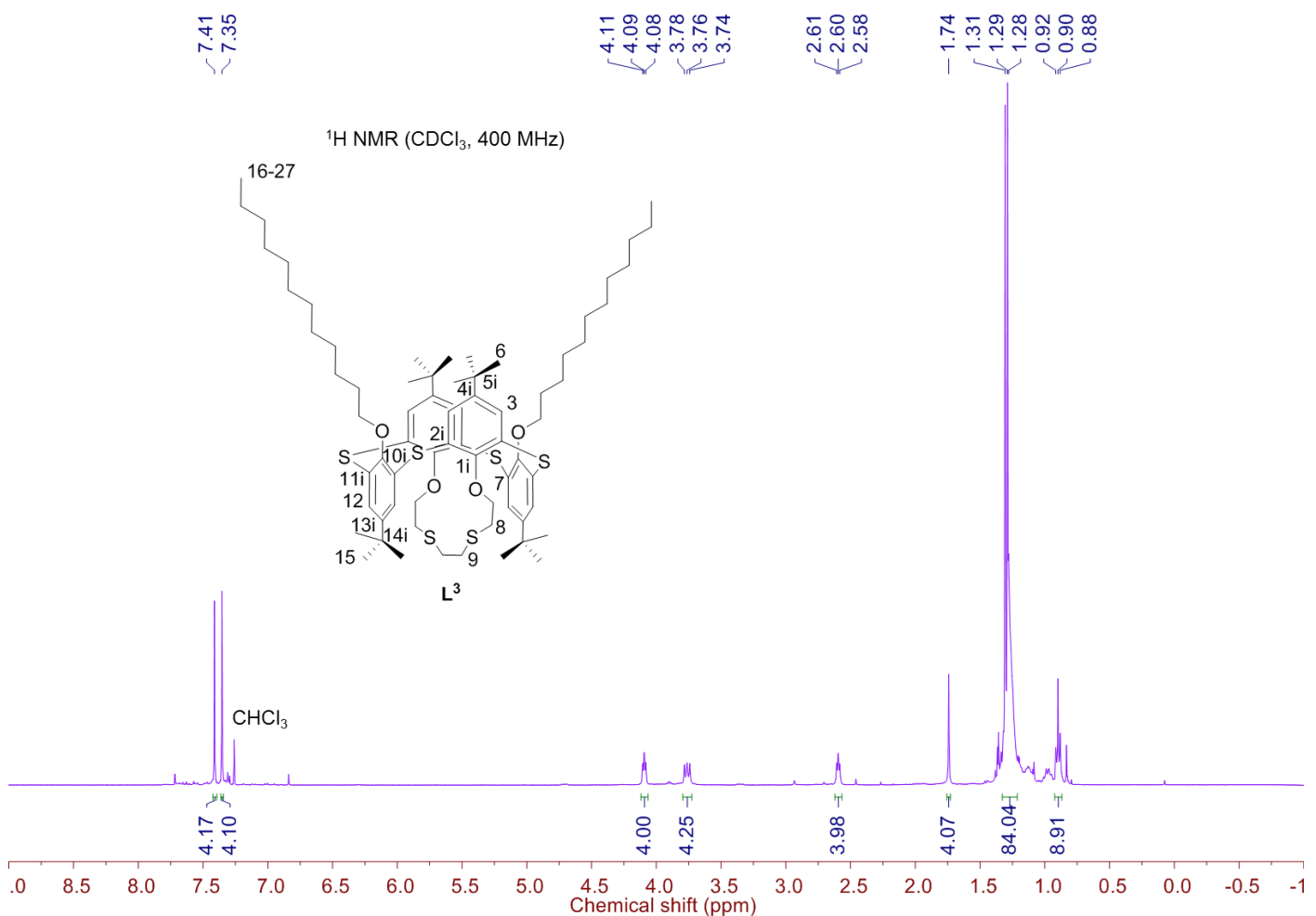


**Figure S1.** <sup>1</sup>H NMR spectrum of compound  $\text{L}^3$  ( $\text{CDCl}_3$ , 400 MHz, 303 K).

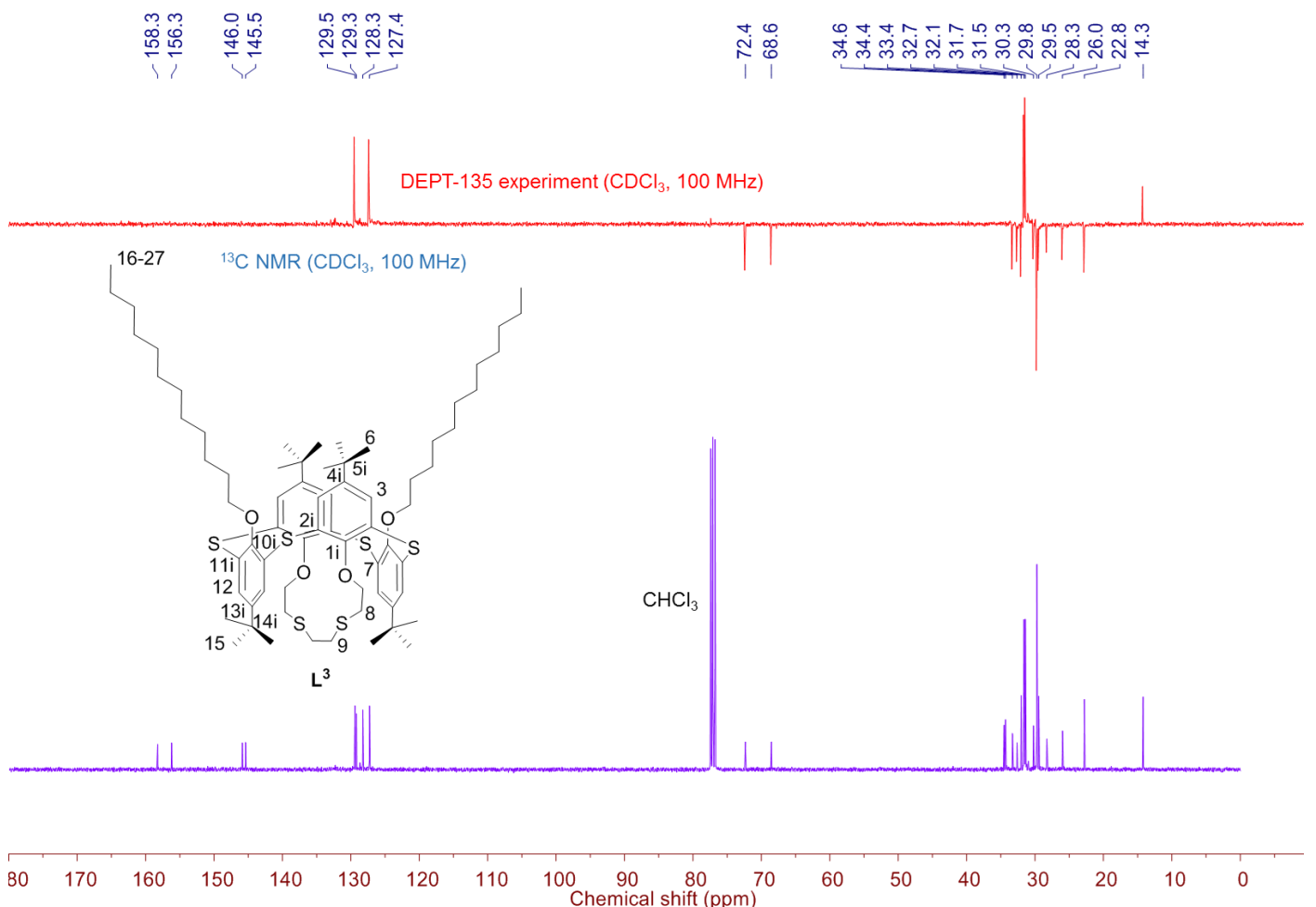


**Figure S2.** <sup>13</sup>C NMR spectrum and DEPT-135 experiment of compound  $\text{L}^3$  ( $\text{CDCl}_3$ , 100 MHz, 303 K).

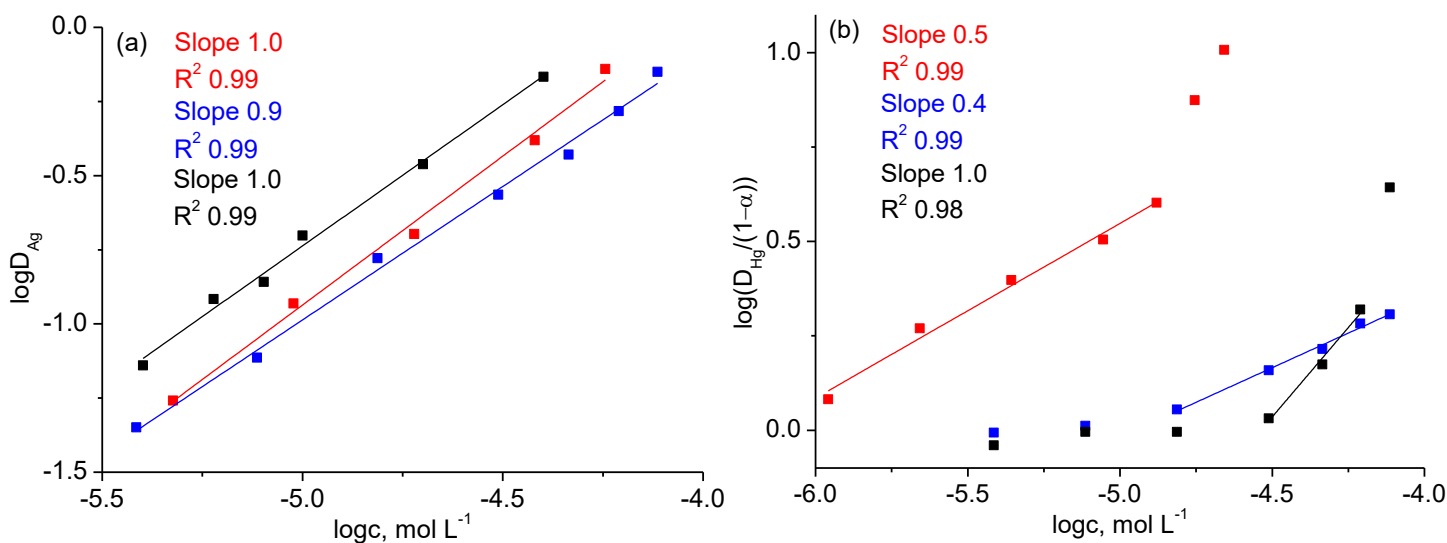


**Figure S3.** Plots of (a)  $\log D_{Ag}$  and (b)  $\log(D_{Hg}/(1-\alpha))$  against  $\log c$  for thioethers  $L^2$  (red line),  $L^3$  (blue line), and  $L^4$  (black line) in the DCM–H<sub>2</sub>O system ( $c(AgPic) = 1 \times 10^{-4} M$  and  $c(HgPic_2) = 1 \times 10^{-4} M$  (ligand  $L^2$ ) or  $5 \times 10^{-5} M$  (ligands  $L^3$  and  $L^4$ ).

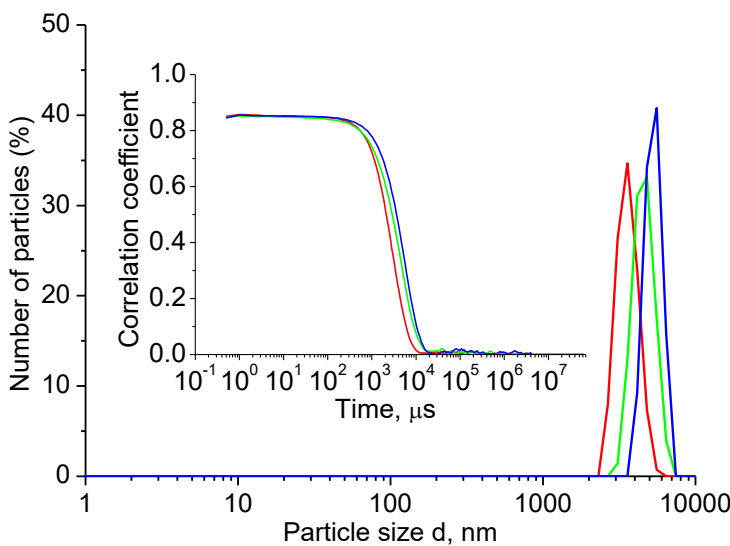


**Figure S4.** Number-averaged particle size distribution and corresponding correlograms of  $CH_2Cl_2$  phase after mixing with aqueous phase containing  $Hg(NO_3)_2$  dissolved in tris-HCl buffer in picric acid (blue curves) and  $CH_2Cl_2$  phase with dissolved compound  $L^2$  after mixing with aqueous phase containing picric acid and tris-HCl buffer (red curve) and aqueous phase containing  $Hg(NO_3)_2$  (green curve).

**Table S1.** Crystallographic parameters of the metal complexes

Formula	$[Ag_2L^2](ClO_4)_2$ , $C_{92}H_{120}Ag_2O_8S_{12}$ , 2(ClO <sub>4</sub> )	$[Ag_2L^2(ClO_4)_2]_n$ , $C_{46}H_{60}Ag_2Cl_2O_{12}S_6$ , 2(CHCl <sub>3</sub> )	$[Hg_2L^4Cl_4]$ , $C_{92}H_{116}Cl_4Hg_2O_8S_{12}$
Molecular weight	2153.23	1522.67	2277.54
Crystal system	triclinic	orthorhombic	triclinic
Space group	<i>P</i> -1	<i>Pbca</i>	<i>P</i> -1
<i>a</i> (Å)	12.200(2)	18.075(4)	10.115(2)
<i>b</i> (Å)	15.200(3)	19.726(4)	15.338(3)
<i>c</i> (Å)	16.680(3)	35.121(7)	19.017(4)
$\alpha$ (deg)	76.01(3)	90	96.48(3)
$\beta$ (deg)	77.06(3)	90	101.05(3)
$\gamma$ (deg)	75.59(3)	90	99.55(3)
<i>V</i> (Å <sup>3</sup> )	2862.5(12)	12522(4)	2823.4(11)
<i>Z</i>	1	8	1
Colour	Colourless	Colourless	Colourless
Crystal dim (mm <sup>3</sup> )	0.03 x 0.02 x 0.02	0.03 x 0.02 x 0.02	0.03 x 0.02 x 0.02
<i>D</i> <sub>calc</sub> (gcm <sup>-3</sup> )	1.249	1.615	1.339
F(000)	1120	6176	7180
$\mu$ (mm <sup>-1</sup> )	0.740	1.333	0.632
Wavelength (Å)	0.7450	0.7450	0.80246
Number of data measurements	48689	129153	44088

Number of data with $I > 2\sigma(I)$	15666 [R(int) = 0.0420]	17272 [R(int) = 0.0410]	12340 [R(int) = 0.1087]
R (%)	5.43	3.08	8.01
$R_w$ (%)	15.84	8.41	22.27
GOF	1.042	1.078	1.036
Largest diff. peak and hole ( $\text{e}\text{\AA}^{-3}$ )	1.380 and -1.683	1.700 and -1.382	2.424 and -2.555

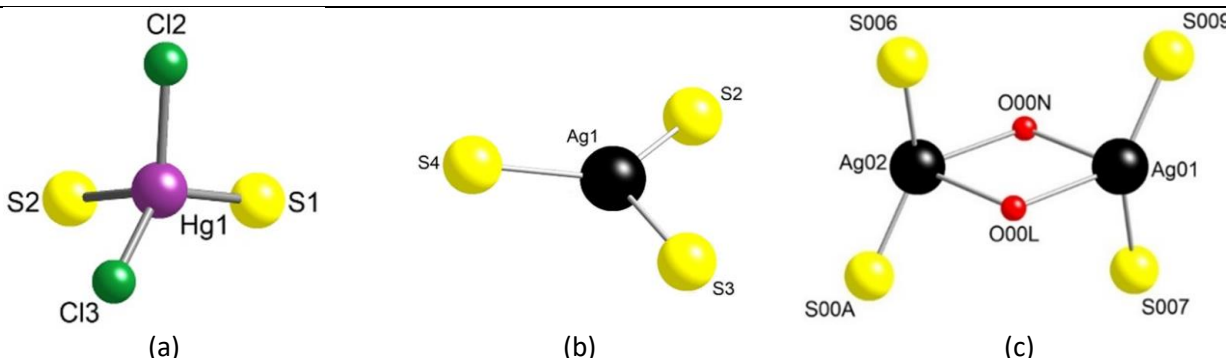


**Figure S5.** Coordination environment of metal ions in (a)  $[\text{Hg}_2\text{L}^4\text{Cl}_4]$ , (b)  $[\text{Ag}_2\text{L}^2_2](\text{ClO}_4)_2$ , and (c)  $[\text{Ag}_2\text{L}^2(\text{ClO}_4)_2]_n$ .

**Table S2.** Bond distances and angles for metal coordination environment in  $[\text{Hg}_2\text{L}^4\text{Cl}_4]$ ,  $[\text{Ag}_2\text{L}^2_2](\text{ClO}_4)_2$ , and  $[\text{Ag}_2\text{L}^2(\text{ClO}_4)_2]_n$

$[\text{Hg}_2\text{L}^4\text{Cl}_4]$	$[\text{Ag}_2\text{L}^2_2](\text{ClO}_4)_2$	$[\text{Ag}_2\text{L}^2(\text{ClO}_4)_2]_n$
$d(\text{Hg1-S1}) = 2.579(8) \text{ \AA}$	$d(\text{Ag1-S2}) = 2.520(6) \text{ \AA}$	$d(\text{Ag01-S007}) = 2.586(7) \text{ \AA}$
$d(\text{Hg1-S2}) = 2.789(5) \text{ \AA}$	$d(\text{Ag1-S3}) = 2.553(1) \text{ \AA}$	$d(\text{Ag01-S009}) = 2.472(1) \text{ \AA}$
$d(\text{Hg1-Cl2}) = 2.397(8) \text{ \AA}$	$d(\text{Ag1-S4}) = 2.570(2) \text{ \AA}$	$d(\text{Ag01-O00L}) = 2.492(2) \text{ \AA}$
$d(\text{Hg1-Cl3}) = 2.340(0) \text{ \AA}$	$\angle \text{S4Ag1S2} = 132.59(7)^\circ$	$d(\text{Ag01-O00N}) = 2.681(8) \text{ \AA}$
$\angle \text{Cl2Hg1S1} = 98.26(3)^\circ$	$\angle \text{S2Ag1S3} = 115.00(0)^\circ$	$d(\text{Ag02-S00A}) = 2.480(2) \text{ \AA}$
$\angle \text{S1Hg1Cl3} = 127.51(2)^\circ$	$\angle \text{S3Ag1S4} = 112.03(7)^\circ$	$d(\text{Ag02-S006}) = 2.585(6) \text{ \AA}$
$\angle \text{Cl3Hg1S2} = 101.22(6)^\circ$		$d(\text{Ag02-O00L}) = 2.739(3) \text{ \AA}$
$\angle \text{S2Hg1Cl2} = 102.03(8)^\circ$		$d(\text{Ag02-O00N}) = 2.514(2) \text{ \AA}$
$\angle \text{Cl2Hg1Cl3} = 130.54(5)^\circ$		$\angle \text{S009Ag01O00N} = 91.02(2)^\circ$
$\angle \text{S1Hg1S2} = 83.00(4)^\circ$		$\angle \text{O00NAG01O00L} = 71.55(0)^\circ$
		$\angle \text{O00LAG01S007} = 91.37(0)^\circ$
		$\angle \text{S007Ag01S009} = 135.38(6)^\circ$
		$\angle \text{S007Ag01O00N} = 91.32(0)^\circ$
		$\angle \text{S009Ag01O00L} = 131.23(4)^\circ$
		$\angle \text{S006Ag02O00N} = 90.72(4)^\circ$
		$\angle \text{S006Ag02O00L} = 88.10(6)^\circ$
		$\angle \text{O00NAG02O00L} = 70.26(0)^\circ$
		$\angle \text{O00LAG02S00A} = 91.84(4)^\circ$
		$\angle \text{S00AAg02S006} = 135.73(0)^\circ$
		$\angle \text{S00AAg02O00N} = 130.58(7)^\circ$
		$\angle \text{Ag01O00NAG02} = 109.67(2)^\circ$
		$\angle \text{Ag01O00LAG02} = 108.51(9)^\circ$

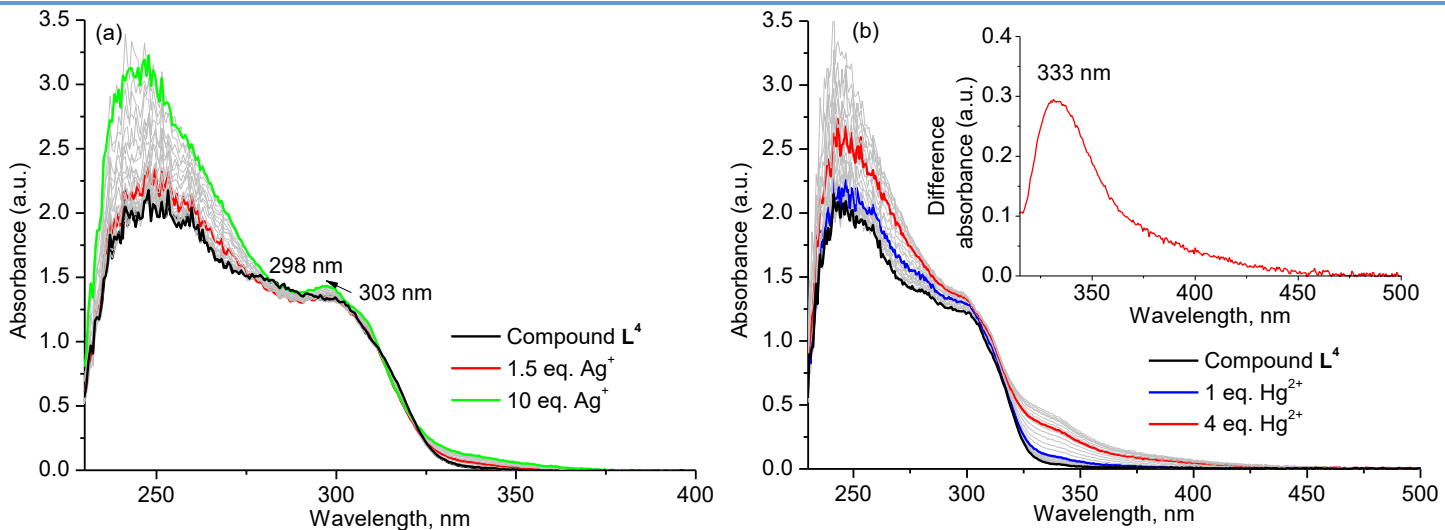


**Figure S6.** Evolution of UV/Vis absorption spectra of compound  $\text{L}^4$  ( $c = 1 \times 10^{-5} \text{ M}$  in 10:1  $\text{CH}_2\text{Cl}_2-\text{MeOH}$ ) on addition of (a)  $\text{Ag}^+$  and (b)  $\text{Hg}^{2+}$  as perchlorates. Inset shows difference spectrum of ligand  $\text{L}^4$  and its  $\text{Hg}$  complex.

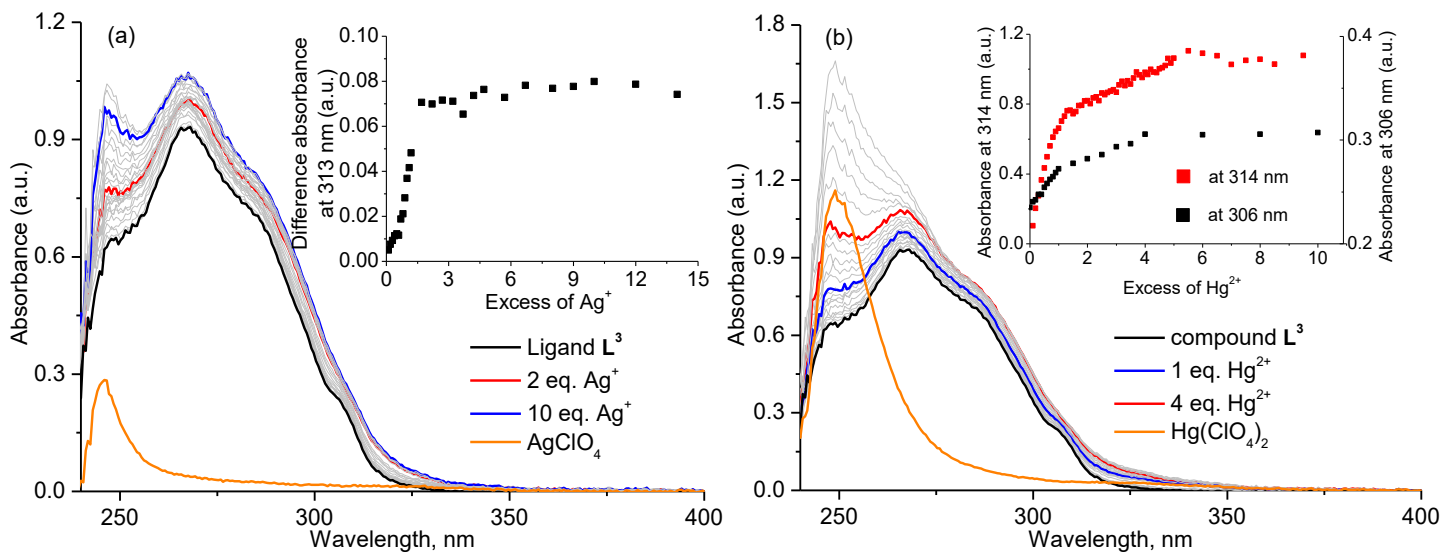


**Figure S7.** Evolution of UV/Vis absorption spectra of compound  $\text{L}^3$  ( $c = 1 \times 10^{-5} \text{ M}$  in 10:1  $\text{CH}_2\text{Cl}_2$ -MeOH) on addition of  $\text{Ag}^+$  and  $\text{Hg}^{2+}$  as perchlorates. Insets show scatter plots of titration.

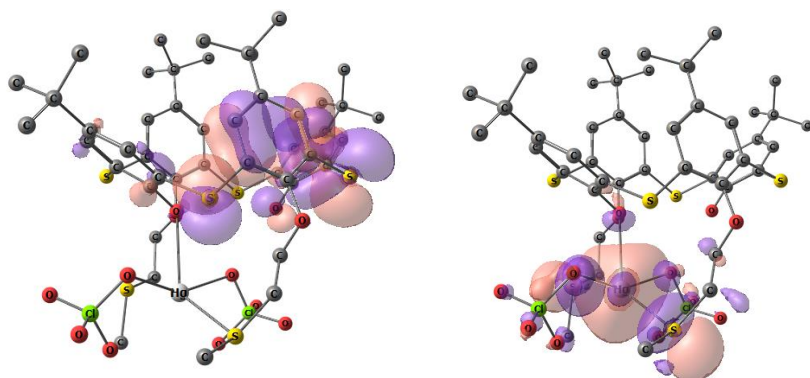


**Figure S8.** Frontier molecular orbitals contributing to low-energy absorption bands of  $\text{L}^2\text{-Hg-a}$  complex: HOMO (left) and LUMO (right).

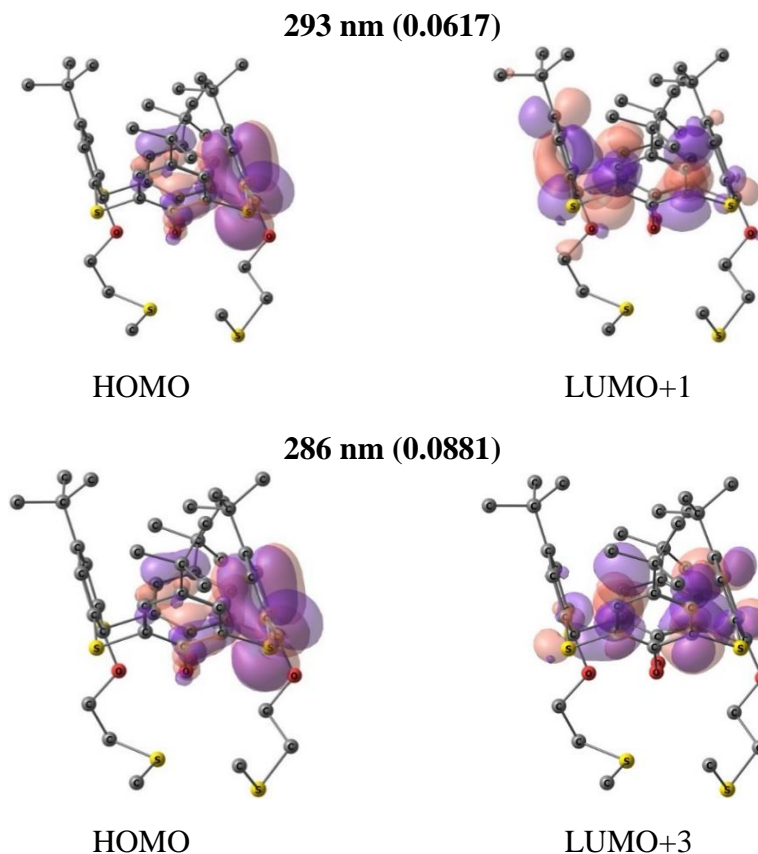


**Figure S9.** Frontier molecular orbitals contributing to low-energy absorption bands of ligand  $\text{L}^2$ .

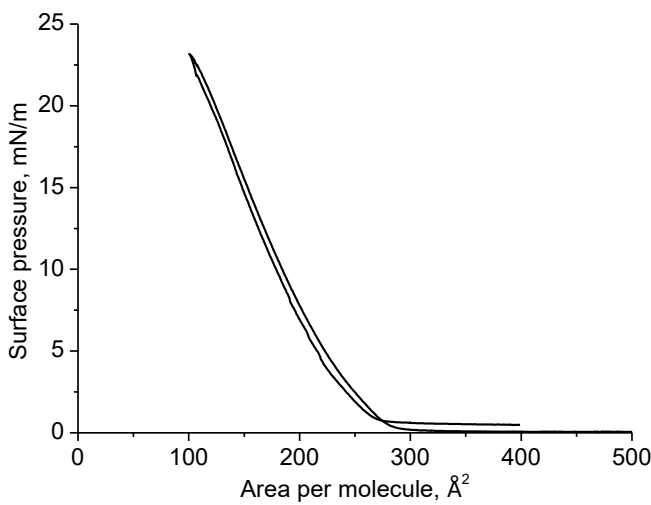


**Figure S10.** Monolayer compression–expansion cycle of compound  $\mathbf{L}^4$  at the air–water interface ( $c = 5 \times 10^{-5} M$  in  $\text{CHCl}_3$ ).

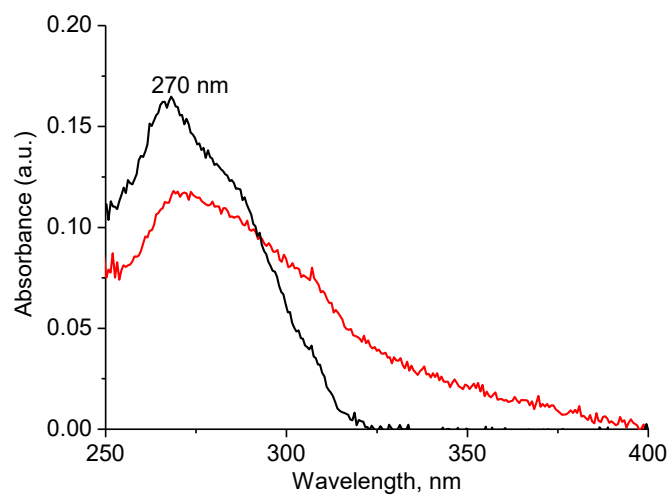


**Figure S11.** UV/Vis spectra of compound  $\mathbf{L}^3$  in  $\text{CHCl}_3$  ( $c = 2 \times 10^{-6} M$ ) (black curve) and at air–water interface ( $\pi = 17 \text{ mN/m}$ ) (red curve).

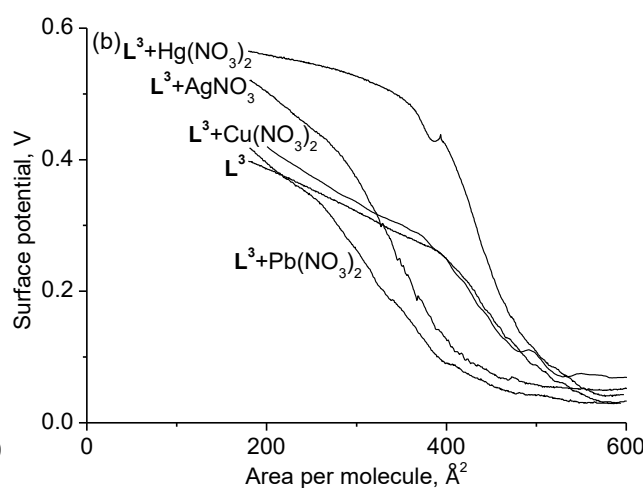
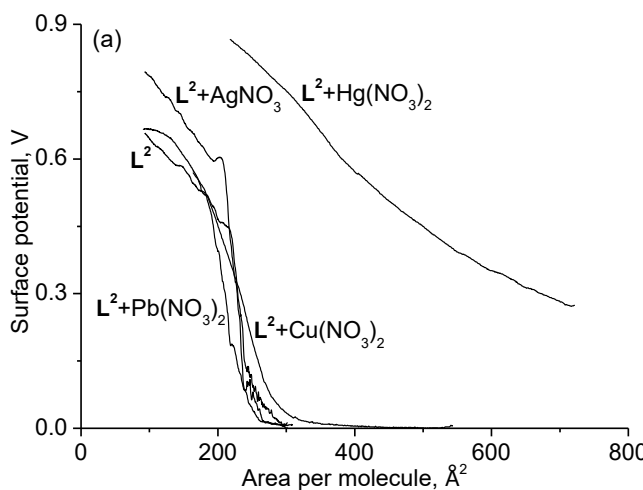


**Figure S12.** SPOT–A isotherms of ligands (a)  $\mathbf{L}^2$  and (b)  $\mathbf{L}^3$  ( $c = 5 \times 10^{-5} M$  in  $\text{CHCl}_3$ ) over deionized water or salt solution.

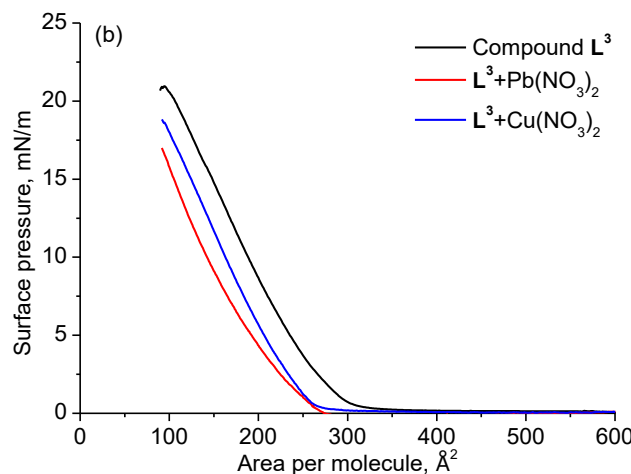
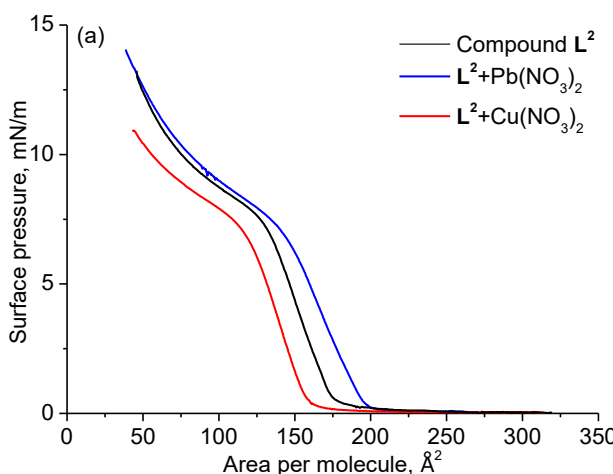


**Figure S13.**  $\pi$ – $A$  isotherms of ligands  $\mathbf{L}^2$  and  $\mathbf{L}^3$  over deionized or salt water subphase ( $c = 5 \times 10^{-5} M$  in  $\text{CHCl}_3$ ).

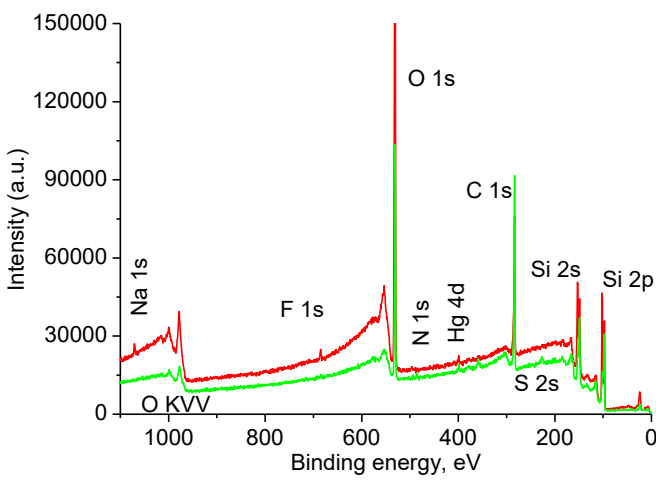


**Table S3.** Main characteristics of the components of XPS spectrum of Langmuir–Blodgett film-coated quartz

Name, state	Position, eV	Intensity, a.u.	FWHM, eV
Si <sup>2p<sub>3/2</sub></sup> , Si <sup>0</sup>	99.34	8410	0.60
Si <sup>2p<sub>1/2</sub></sup> , Si <sup>0</sup>	99.95	4205	0.50
Si <sup>+</sup>	100.30	1657	0.84
Hg <sup>4f<sub>7/2</sub></sup>	101.16	2910	1.18
Si <sup>2+</sup>	101.86	940	0.97
Si <sup>4+</sup>	103.20	8173	1.52
Hg <sup>4f<sub>5/2</sub></sup>	105.42	2216	1.19

**Figure S14.** XPS spectra of bare quartz (red curve) and LB film on quartz formed by monolayer of compound **L<sup>3</sup>** over 10<sup>-4</sup> M Hg(ClO<sub>4</sub>)<sub>2</sub> solution (green curve).

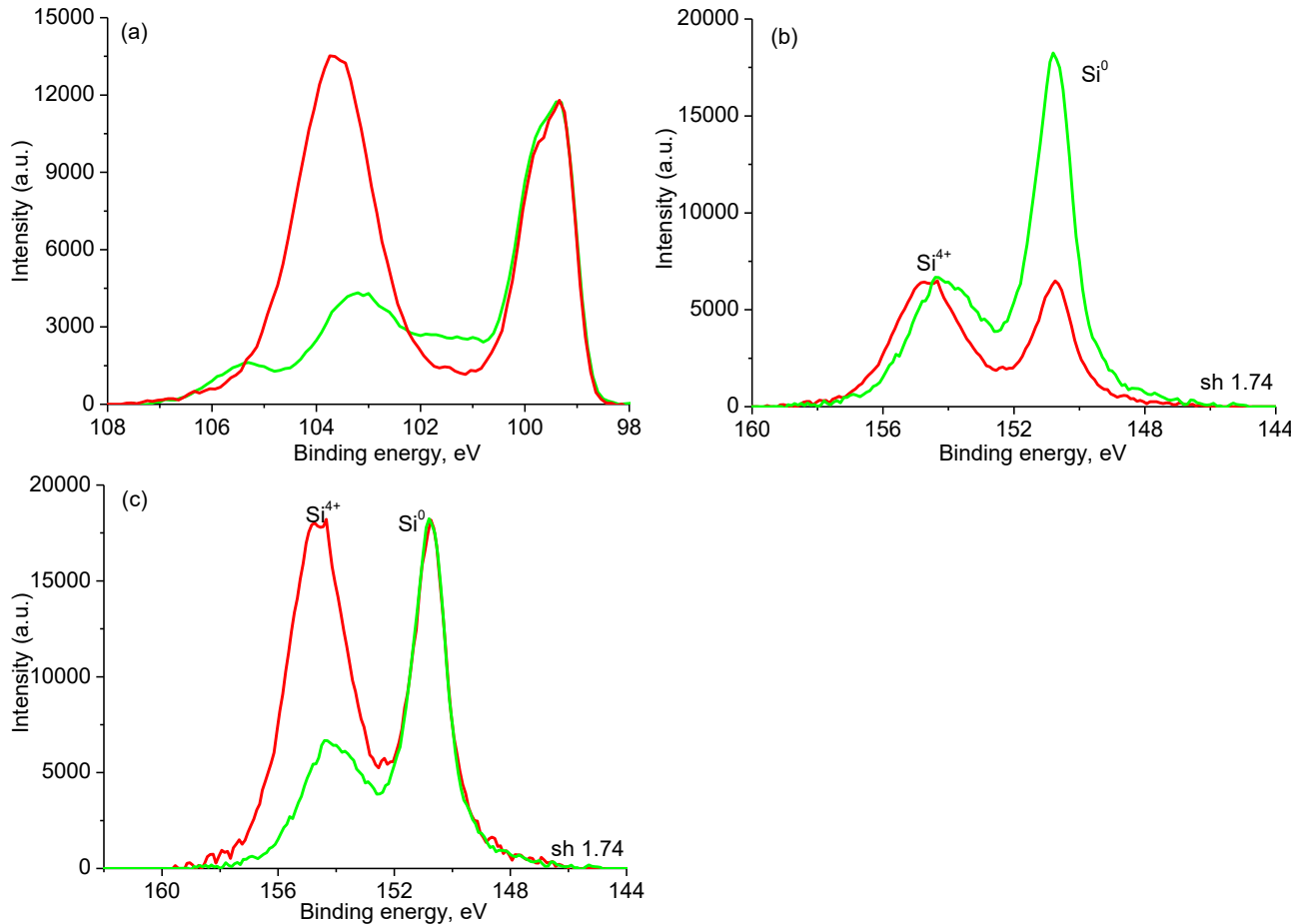


**Figure S15.** Partial XPS spectra of (a) Si2p and (b,c) Si2s regions of bare quartz (red curve) and LB film of compound **L<sup>3</sup>** with Hg(ClO<sub>4</sub>)<sub>2</sub> (green curve) normalized by the intensity of (a,c) low- and (b) high-energy peaks.